



## OPEN ACCESS

## EDITED BY

Gaoxiang Ouyang,  
Beijing Normal University, China

## REVIEWED BY

Kapil Gururangan,  
University of California, Los Angeles,  
United States

Jia Zhao,  
Southwest University, China  
Kusumika Krori Dutta,  
Ramaiah Institute of Technology, India

## \*CORRESPONDENCE

Hunmin Kim  
✉ [hunminkim@snuh.org](mailto:hunminkim@snuh.org)

RECEIVED 22 February 2024

ACCEPTED 03 May 2024

PUBLISHED 20 May 2024

## CITATION

Chung YG, Cho A, Kim H and Kim KJ (2024)  
Single-channel seizure detection with clinical  
confirmation of seizure locations using  
CHB-MIT dataset.  
*Front. Neurol.* 15:1389731.  
doi: 10.3389/fneur.2024.1389731

## COPYRIGHT

© 2024 Chung, Cho, Kim and Kim. This is an  
open-access article distributed under the  
terms of the [Creative Commons Attribution  
License \(CC BY\)](https://creativecommons.org/licenses/by/4.0/). The use, distribution or  
reproduction in other forums is permitted,  
provided the original author(s) and the  
copyright owner(s) are credited and that the  
original publication in this journal is cited, in  
accordance with accepted academic  
practice. No use, distribution or reproduction  
is permitted which does not comply with  
these terms.

# Single-channel seizure detection with clinical confirmation of seizure locations using CHB-MIT dataset

Yoon Gi Chung<sup>1</sup>, Anna Cho<sup>1</sup>, Hunmin Kim<sup>1,2\*</sup> and Ki Joong Kim<sup>3</sup>

<sup>1</sup>Department of Pediatrics, Seoul National University Bundang Hospital, Seoul National University College of Medicine, Seongnam-si, Gyeonggi-do, Republic of Korea, <sup>2</sup>Department of Pediatrics, Seoul National University College of Medicine, Seoul, Republic of Korea, <sup>3</sup>Department of Pediatrics, Seoul National University Children's Hospital, Seoul National University College of Medicine, Seoul, Republic of Korea

**Introduction:** Long-term electroencephalography (EEG) monitoring is advised to patients with refractory epilepsy who have a failure of anti-seizure medication and therapy. However, its real-life application is limited mainly due to the use of multiple EEG channels. We proposed a patient-specific deep learning-based single-channel seizure detection approach using the long-term scalp EEG recordings of the Children's Hospital Boston-Massachusetts Institute of Technology (CHB-MIT) dataset, in conjunction with neurologists' confirmation of spatial seizure characteristics of individual patients.

**Methods:** We constructed 18-, 4-, and single-channel seizure detectors for 13 patients. Neurologists selected a specific channel among four channels, two close to the behind-the-ear and two at the forehead for each patient, after reviewing the patient's distinctive seizure locations with seizure re-annotation.

**Results:** Our multi- and single-channel detectors achieved an average sensitivity of 97.05–100%, false alarm rate of 0.22–0.40/h, and latency of 2.1–3.4 s for identification of seizures in continuous EEG recordings. The results demonstrated that seizure detection performance of our single-channel approach was comparable to that of our multi-channel ones.

**Discussion:** We suggest that our single-channel approach in conjunction with clinical designation of the most prominent seizure locations has a high potential for wearable seizure detection on long-term EEG recordings for patients with refractory epilepsy.

## KEYWORDS

deep learning, electroencephalography, epilepsy, seizure detection, single channel, wearable

## 1 Introduction

Epilepsy is a chronic neurological condition with a worldwide prevalence of 0.64% (1). The major symptom of epilepsy is seizures, and it is characterized by unprovoked and unexpected abnormal brain activity due to neuronal hyperexcitability and hypersynchrony (2). Approximately one-third of epileptic patients are suffering from refractory epilepsy (3, 4). Electroencephalography (EEG) is a critical initial step in the diagnosis of epilepsy owing to its powerful ability to uncover electrophysiological evidence of epileptic brain activity (5). As patients with refractory epilepsy tend to be exposed to injuries, psychosocial impairment, which seriously deteriorates their quality of life,

or even death (6, 7), long-term EEG monitoring is essential for managing seizures and establishing appropriate treatment strategies (8–10). However, manual detection of seizures in long-term EEG recordings is highly time-consuming, labor-intensive, and clinician-dependent, and it often leads to misidentification and overmedication (11, 12).

Numerous automated seizure detection approaches based on machine and deep learning techniques have been proposed to overcome the burden of manual seizure detection (11, 13). Recently, many studies have adopted convolutional neural networks (CNN), recurrent neural networks (RNN), and hybrid CNN-RNN architectures for deep learning-based automated seizure detection approaches, with high performance in the identification of seizures on the scalp and intracranial EEG recordings. Despite the remarkable advancements in automated seizure detection, its real-life application for patients with refractory epilepsy is still limited because most approaches require multiple EEG channels, typically  $\geq 18$  for scalp EEG electrodes, to acquire sufficient amount of data in hospital environments. The use of multiple EEG electrodes makes patients uncomfortable and induces high computational complexity, particularly during long-term EEG monitoring.

Some studies on deep learning-based automated seizure detection have proposed various methods to reduce the number of EEG channels for patient-friendly and efficient machine-based examination of the occurrence of seizures on long-term scalp EEG recordings. They reported high seizure detection performance with reduced montage settings of at least two EEG channels, comparable to those with a full montage setting (14–23). In addition, some recent studies on machine (24–27) and deep learning-based (28) seizure detection approaches have utilized four behind-the-ear EEG channels. They demonstrated the feasibility of using a small number of channels for automated seizure detection in the long-term wearable EEG recordings of patients with refractory epilepsy. However, the approaches based on behind-the-ear channels are expected to mostly focused on seizures, predominantly in regions near the temporal lobes.

Seizure detection with single-channel EEG monitoring is the most convenient approach for patients who use wearable devices for long durations daily. Using one channel is expected to considerably enhance comfort and reduce complexity during long-term EEG monitoring. A recent study proposed a wearable approach for EEG acquisition using a device in the ear called ear-EEG and demonstrated its ability to detect electroencephalographic patterns of seizures in the temporal lobe (29). Other recent studies proposed a single-channel EEG sensor called Epilog, which could be easily attached to hairless regions such as the forehead or behind each ear (30, 31). They demonstrated that epileptologists and machine learning-based algorithms could competently identify focal seizures with single-channel EEG monitoring if the sensors were placed near the seizure onset foci. Based on these studies, using one channel is expected to guarantee automated identification of seizures during wearable EEG monitoring, at least for seizures near their locations on the scalp.

In this study, we proposed a deep learning-based patient-specific single-channel seizure detection approach in conjunction with clinical designation of the most prominent seizure locations. We built (1) 18-channel seizure detectors with a full-montage setting, (2) 4-channel detectors whose channel locations were fixed onto the forehead and behind both ears, and (3) single-channel detectors whose channels were selected based on neurologists' confirmation of the spatial seizure characteristics of individual patients. Subsequently,

we compared the seizure detection capabilities of single-channel detectors with those of multi-channel detectors to evaluate the practical usefulness of our single-channel approach for long-term wearable seizure detection.

## 2 Methods

### 2.1 Dataset

We used the Children's Hospital Boston-Massachusetts Institute of Technology (CHB-MIT) scalp EEG database.<sup>1</sup> This dataset consisted of scalp EEG recordings from 22 pediatric participants (5 males, aged 3–22, 17 females, aged 1.5–19). All EEG recordings were grouped into 23 cases from chb01 to chb23 (chb01 and chb21 were the same participants but chb21 was obtained 1.5 years later; chb24 was excluded from this study). Each case had 9–42 European data format (EDF) files sampled at 256 Hz with a 16-bit resolution. The EDF files had 1–4 recording hours with 23–26 channels, in accordance with the international 10–20 system. Herein, a total of 182 seizures were annotated in the publicly available EDF files of the 23 cases. As three EDF files of chb12 did not have longitudinal bipolar montages, their corresponding 13 seizures were excluded. In total, we obtained 169 seizures in the 23 cases. Each case represents an individual patient. The Institutional Review Board of Seoul National University Bundang Hospital approved this study (No. B-2205-758-105) and waived the requirement for informed consent due to the retrospective nature of the study. This study was conducted following the principles of the Declaration of Helsinki.

We selected 18 channels, namely Fp1-F3, F3-C3, C3-P3, P3-O1, Fp2-F4, F4-C4, C4-P4, P4-O2, Fp1-F7, F7-T7, T7-P7, P7-O1, Fp2-F8, F8-T8, T8-P8, P8-O2, Fz-Cz, and Cz-Pz, as a full montage setting. Subsequently, we selected four channels, Fp1-F3, Fp2-F4, P7-O1, and P8-O2, from the full montage setting. Two channels, P7-O1 and P8-O2, were selected because they were closest to the behind-the-ear positions. The other two channels, Fp1-F3 and Fp2-F4, were selected because they were placed on the forehead. These four channels were selected because they were expected to be the most common positions for wearable electrodes to be easily attached.

Two neurologists reviewed all seizures in the 23 cases to determine their distinctive locations representing spatial seizure characteristics on the scalp, such as the frontal, temporal, parietal, and occipital regions. As they reviewed only electrographic seizures without video data, seizure locations of six cases could not be identified (chb12, chb14, chb16, chb18, chb20, and chb21), and those of four cases were not close to Fp1-F3, Fp2-F4, P7-O1, or P8-O2 (chb06, chb09, chb13, and chb19). Therefore, they selected 13 cases whose seizure locations were identifiable by four or one of the four channels. Detailed information of the 13 cases is presented in Table 1.

Ictal period was defined as the interval between seizure onset and termination, and interictal period was defined as the remaining section after excluding all ictal periods. The neurologists re-annotated the ictal periods corresponding to 77 seizures of the 13 cases based on their confirmation of distinctive seizure locations to make the periods contain ictal EEG characteristics as clear as possible. They were

<sup>1</sup> <https://physionet.org/content/chbmit/1.0.0/>

TABLE 1 Patient information on the 13 cases of the CHB-MIT dataset.

| Case      | Age (yr)   | Sex | Number of seizures | Seizure length (s) | Total seizure length (s) | Recording length (h) | Single-channel |
|-----------|------------|-----|--------------------|--------------------|--------------------------|----------------------|----------------|
| chb01     | 11.0       | F   | 7                  | 50.6 ± 23.0        | 354                      | 40.6                 | P8-O2          |
| chb02     | 11.0       | M   | 3                  | 50.7 ± 36.3        | 152                      | 35.3                 | P7-O1          |
| chb03     | 14.0       | F   | 7                  | 39.3 ± 6.0         | 275                      | 38.0                 | Fp1-F3         |
| chb04     | 22.0       | M   | 4                  | 32.8 ± 16.3        | 131                      | 156.1                | P8-O2          |
| chb05     | 7.0        | F   | 5                  | 71.4 ± 16.1        | 357                      | 39.0                 | P7-O1          |
| chb07     | 14.5       | F   | 3                  | 37.0 ± 7.5         | 111                      | 67.1                 | Fp1-F3         |
| chb08     | 3.5        | M   | 5                  | 42.4 ± 20.4        | 212                      | 20.0                 | Fp1-F3         |
| chb10     | 3.0        | M   | 7                  | 44.1 ± 14.6        | 309                      | 50.0                 | P7-O1          |
| chb11     | 12.0       | F   | 3                  | 46.7 ± 46.2        | 140                      | 34.8                 | P7-O1          |
| chb15     | 16.0       | M   | 20                 | 80.8 ± 46.5        | 1,616                    | 40.0                 | P7-O1          |
| chb17     | 12.0       | F   | 3                  | 78.0 ± 17.8        | 234                      | 21.0                 | P8-O2          |
| chb22     | 9.0        | F   | 3                  | 60.7 ± 11.0        | 182                      | 31.0                 | Fp1-F3         |
| chb23     | 6.0        | F   | 7                  | 49.4 ± 18.5        | 346                      | 26.6                 | Fp1-F3         |
| Total     |            |     | 77                 |                    | 4,419                    | 599.5                |                |
| Mean ± SD | 10.8 ± 5.3 |     | 5.9 ± 4.6          | 57.4 ± 32.9        | 339.9 ± 393.5            | 46.1 ± 35.2          |                |

Seizure length represents mean ± standard deviation (SD) for our re-annotated seizures.

requested to adjust the existing ictal periods (publicly available annotation) to have noticeable electrographic seizure-related EEG variations (re-annotation). Figure 1 shows representative ictal periods with publicly available annotations and our re-annotations.

## 2.2 Preprocessing

All EEG data were bandpass-filtered between 1 and 30 Hz as most rhythmic activities of seizures in scalp EEG recordings could be captured in this frequency band (32, 33). The bandpass-filtered EEG signals in the ictal and interictal periods were divided into 4-s long segments to analyze EEG oscillations from delta (1–4 Hz) to beta (13–30 Hz) bands. The EEG signals were split every one data point (1/256 s, approximately 4 ms) to maximize the number of segments, yielding an overlap of 3.996 s between two consecutive segments. EEG segments from the ictal and interictal periods were defined as the ictal and interictal segments, respectively. The number of interictal segments was much larger than that of ictal segments because the total length of the interictal periods (46.02 ± 35.26 h, averaged over 13 cases) was much longer than that of the ictal periods (0.09 ± 0.11 h). We used a balanced batch generator to create a subset of the dataset for each batch with the same number of randomly selected ictal and interictal segments during model training to handle the imbalanced dataset of ictal and interictal segments. No additional artifact rejection was performed to avoid signal distortion.

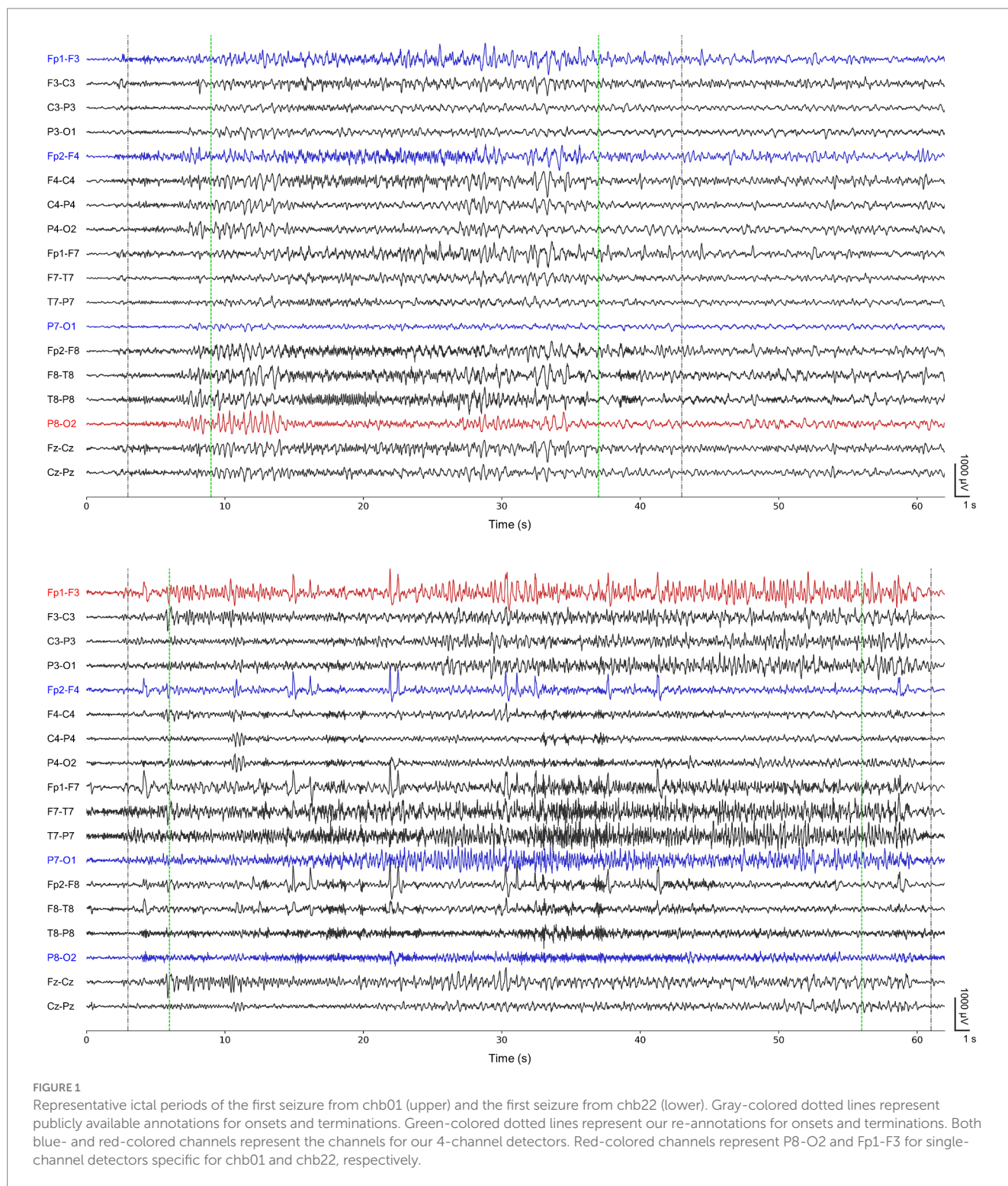
## 2.3 Patient-specific seizure detection

Similar to previous studies on deep learning-based seizure detection (34, 35), we applied *k*-fold cross-validation to train and evaluate our patient-specific seizure detectors, where *k* was the number of EDF files with at least one or more seizures in each case.

First, we gathered interictal segments from all EDF files with no seizure. Next, we gathered ictal segments from *k*-1 EDF files with seizures. These datasets were used to construct a CNN-based binary classification model as a detector for classifying ictal and interictal segments, with a ratio of 7:2:1 for the training, validation, and test datasets (segment-level evaluation). Then, we used the remaining EDF file with seizures to evaluate seizure detection in the continuous EEG recordings. We applied the classification model trained using *k*-1 EDF files to the remaining EDF file to consecutively classify ictal and interictal segments based on the sliding-window technique using 4 s segments overlapping with a step size of 1 s (event-level evaluation). The length and number of seizures of each EDF file for the event-level evaluation varied from one to four and from one to five, respectively, depending on the case. We repeated both the segment- and event-level evaluation steps *k* times for each case.

In the segment-level evaluation, we designated an EEG segment with ictal probability greater than 0.5 as an ictal segment and less than 0.5 as an interictal segment. We used sensitivity, specificity, accuracy, and area under the receiver operating characteristic curve (AUC) as performance measures. We defined sensitivity, specificity, and accuracy as the number of correctly classified ictal segments divided by the number of true ictal segments, the number of correctly classified interictal segments divided by the number of true interictal segments, and the total number of correctly classified segments divided by the number of all test segments, respectively.

In the event-level evaluation, we performed three post-processing steps to acquire model-annotated seizures in the continuous EEG recordings. First, we used a Savitzky–Golay filter (36) with a window length of 10 and polynomial order of 3 to smooth time-varying ictal probability. Second, we collected segments with ictal probability exceeding a certain threshold *Th*. Third, we obtained *L* consecutive segments above the threshold. Any sets of *L* consecutive segments that were less than 10 s apart were merged. *Th* and *L* varied from 0.2 to 0.9 and from 5 to 10, respectively, depending on cases. If there were any



overlaps between the model-annotated seizure and its nearby neurologist-annotated seizure, the model-annotated one was regarded as a correctly detected seizure. If no overlap, the neurologist-annotated one was regarded as a missed seizure. We defined a false alarm as a model-labeled seizure placed outside any neurologist-annotated seizures. We optimized the parameters of the Savitzky–Golay filter to minimize the number of false alarms. Further, we used sensitivity, false alarm rate (FAR), and latency as performance measures.

We defined sensitivity, FAR, and latency as the number of correctly detected seizures divided by the number of neurologist-annotated seizures, number of false alarms divided by the length of the test EEG recording, and the time delay between the onsets of the model- and neurologist-annotated seizures, respectively.

To construct 18-channel detectors, we used 18-channel EEG time series at the full montage setting as input data for the classification models. To construct 4-channel detectors, we used 4-channel EEG

time series from Fp1-F3, Fp2-F4, P7-O1, and P8-O2 as input data for the classification models. To construct single-channel detectors, our neurologists selected one channel based on their confirmation of distinctive seizure locations for each case. They were requested to select one specific channel from the abovementioned four channels. For example, they selected Fp1-F3 if they determined the left-side frontal region to be the most distinctive. Subsequently, we used the single-channel EEG time series as input data for the classification models. Detailed information on the overall process is presented in Figure 2.

## 2.4 CNN architecture

We adopted a stacked two-dimensional (2D) CNN architecture, similar to the one-dimensional (1D) architecture used in the previous study (35), for our binary classification models. We constructed two 2D CNN modules in parallel. Each module consisted of three convolution, batch normalization, and max-pooling layers. As we used multi- or single-channel EEG time series as input, 4 s EEG segments with a size of  $N \times 1,024$  were fed into the input layer, where  $N$  was the number of channels. The convolution layers contained 32, 64, and 128 filters with rectified linear units as their activation functions. One module had a filter size of  $1 \times 3$ , and the other one had a filter size of  $1 \times 5$  with strides of 2, 2, and 1 for three convolution layers. Max-pooling layers had a pooling size of 3. The final layers of the two modules were concatenated into a single feature layer. The concatenated feature vector was flattened by global average pooling and fed into fully connected layers. We obtained an output vector

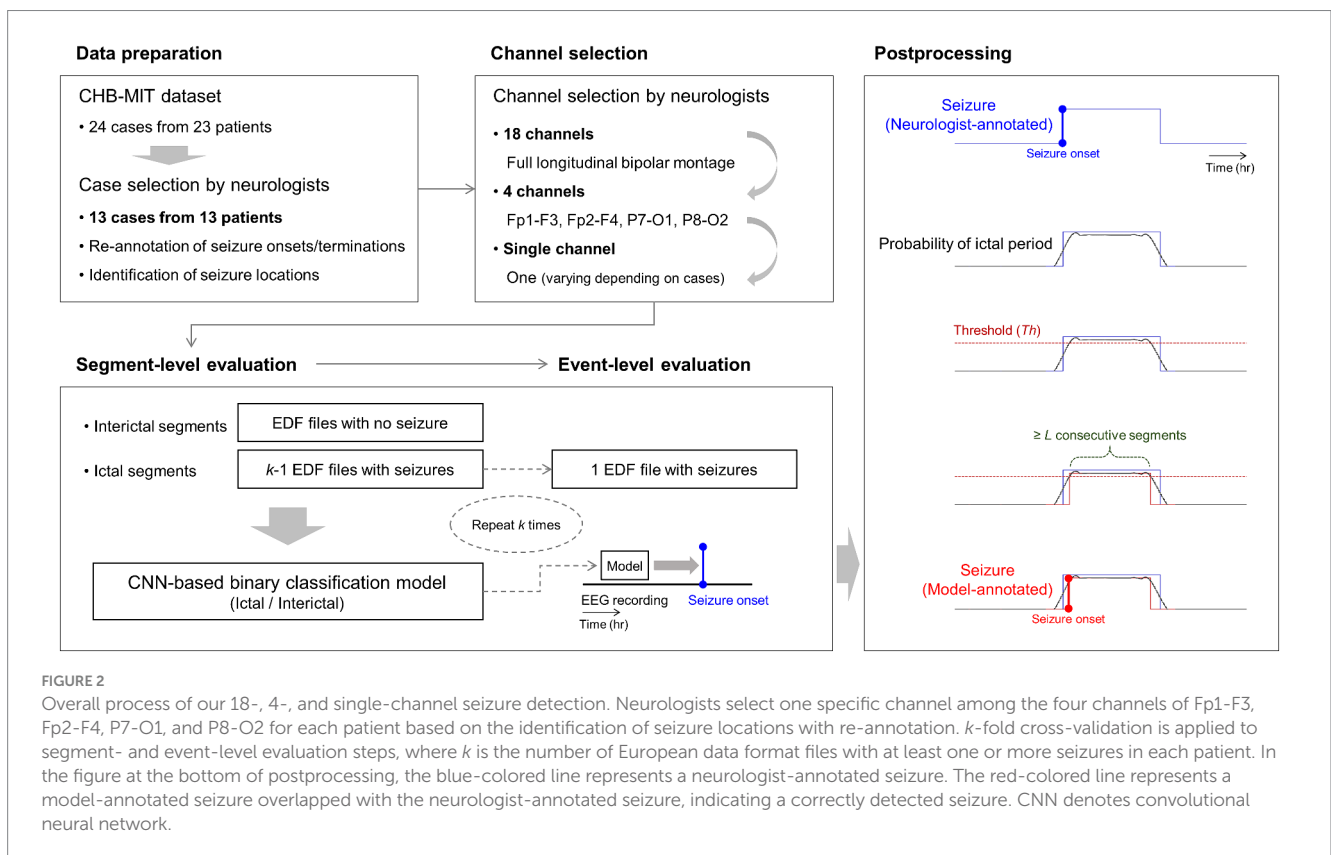
using a softmax function from the fully connected layers with ictal probability ranging from zero to one. An input segment was classified into an ictal one if its ictal probability was  $\geq 0.5$  and interictal one if  $< 0.5$ . We used root mean square propagation with a learning rate of  $3 \times 10^{-4}$  as an optimizer, binary cross-entropy as a loss function, and early stopping with a patience of 15 to avoid overfitting. We used Python 3.8, TensorFlow 2.2, compute unified device architecture (CUDA) 10.1, and four NVIDIA TITAN V graphic cards with 12 GB of memory. Detailed information on the CNN architecture is presented in Figure 3.

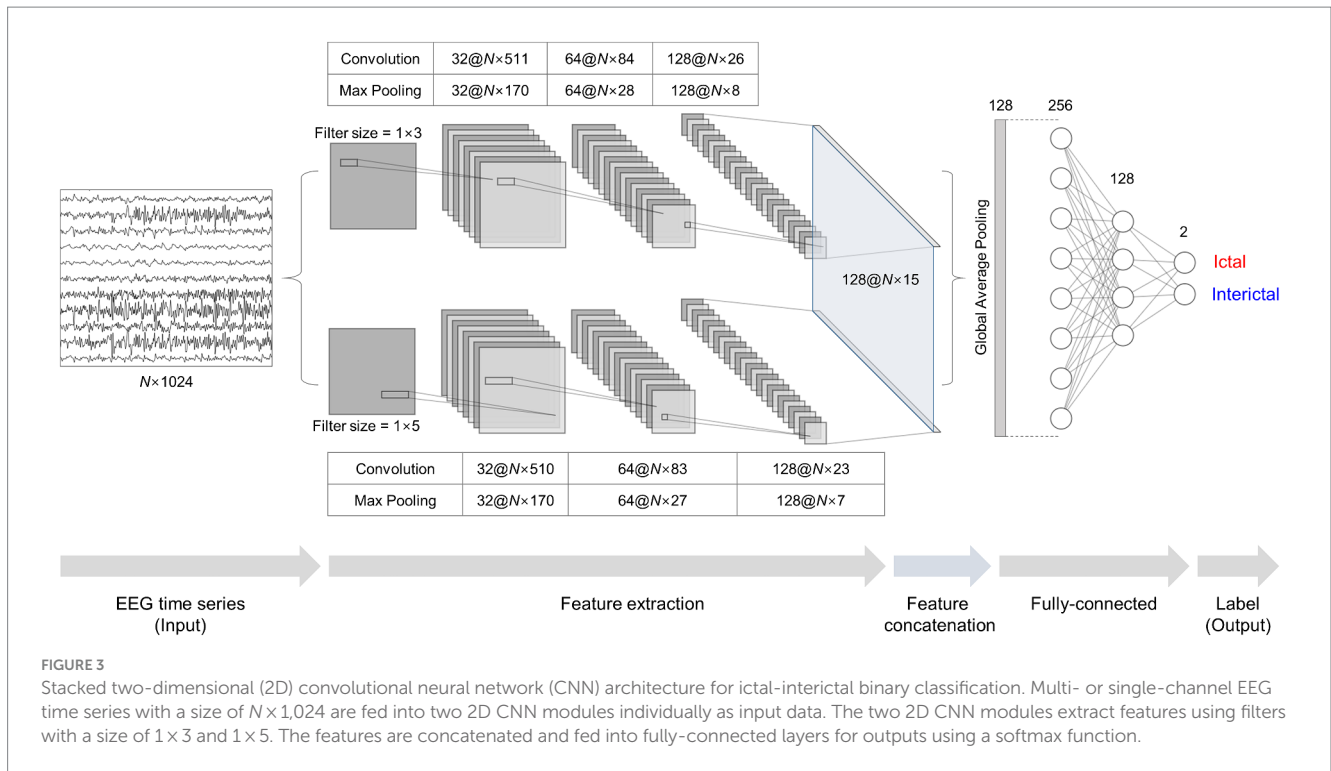
## 3 Results

### 3.1 18-channel seizure detection

We observed the ictal-interictal binary classification performance of our patient-specific 18-channel seizure detectors in the segment-level evaluation, with a sensitivity, specificity, accuracy, and AUC of  $98.66 \pm 1.19\%$  (mean  $\pm$  standard deviation),  $98.47 \pm 2.71\%$ ,  $98.47 \pm 2.69\%$ , and  $98.56 \pm 1.81\%$ , respectively, averaged over the 13 cases. Among the 13 cases, chb02 and chb04 exhibited the highest accuracy of  $99.97 \pm 0.03\%$  and  $99.97 \pm 0.02\%$ , respectively (sensitivity and specificity of  $98.12 \pm 3.25\%$  and  $99.97 \pm 0.03\%$ ;  $98.18 \pm 2.52\%$  and  $99.97 \pm 0.02\%$ , respectively). However, chb15 exhibited the lowest accuracy of  $90.33 \pm 8.93\%$  ( $96.20 \pm 5.32\%$  and  $90.24 \pm 9.13\%$ , respectively), averaged over  $k$ -fold cross-validation.

We observed the seizure-detection performance of the 18-channel detectors in the event-level evaluation with a sensitivity, FAR, and





latency of 100%,  $0.30 \pm 0.47/h$ , and  $2.1 \pm 6.7s$ , averaged over the 13 cases, respectively. The 18-channel seizure detection exhibited a mean number of correctly detected seizures, missed seizures, and false alarms of  $5.9 \pm 4.6$ , 0, and  $2.4 \pm 4.4$ , respectively, during a mean length of EEG recordings of  $7.0 \pm 4.1h$ . All patients exhibited 100% sensitivity. However, chb11 and chb15 exhibited FAR of 1.43/h and 1.14/h, respectively, thus indicating more than one false alarm per hour.

### 3.2 4-channel seizure detection

The ictal-interictal binary classification performance of our patient-specific 4-channel seizure detectors in the segment-level evaluation had a sensitivity, specificity, accuracy, and AUC of  $97.31 \pm 3.78\%$ ,  $97.72 \pm 3.61\%$ ,  $97.73 \pm 3.59\%$ , and  $97.51 \pm 2.94\%$ , respectively, averaged over the 13 cases. Among the 13 cases, chb04 and chb05 exhibited the highest accuracy of  $99.92 \pm 0.07\%$  and  $99.92 \pm 0.06\%$ , respectively (sensitivity and specificity of  $93.75 \pm 10.83\%$  and  $99.92 \pm 0.07\%$ ;  $99.69 \pm 0.70\%$  and  $99.92 \pm 0.06\%$ , respectively). However, chb15 exhibited the lowest accuracy of  $87.93 \pm 10.51\%$  (sensitivity and specificity of  $92.80 \pm 9.47\%$  and  $87.86 \pm 10.79\%$ , respectively) averaged over  $k$ -fold cross-validation.

We observed the seizure detection performance of the 4-channel detectors in the event-level evaluation with a sensitivity, FAR, and latency of  $97.05 \pm 9.23\%$ ,  $0.40 \pm 0.77/h$ , and  $3.5 \pm 4.8s$ , averaged over the 13 cases. The 4-channel seizure detection exhibited a mean number of correctly detected seizures, missed seizures, and false alarms of  $5.8 \pm 4.4$ ,  $0.2 \pm 0.4$ , and  $2.9 \pm 6.1$ , respectively, during a mean length of EEG recordings of  $7.0 \pm 4.1h$ . Among the 13 cases, chb11 and chb15 exhibited a FAR of 2.51/h and 1.57/h, respectively, whereas chb17 exhibited the lowest sensitivity (66.67%) with no false alarm.

### 3.3 Single-channel seizure detection

Among the channels in our 4-channel seizure detection approach, the left frontal one (Fp1-F3) was assigned to five cases of chb03, chb07, chb08, chb22, and chb23; the left parieto-occipital one (P7-O1) to five cases of chb02, chb05, chb10, chb11, and chb15; and the right parieto-occipital one (P8-O2) to three cases of chb01, chb04, and chb17. No cases were assigned to the right frontal channel (Fp2-F4).

The ictal-interictal binary classification performance of our patient-specific single-channel seizure detectors in the segment-level evaluation had a sensitivity, specificity, accuracy, and AUC of  $96.76 \pm 3.97\%$ ,  $98.19 \pm 1.82\%$ ,  $98.18 \pm 1.83\%$ , and  $97.47 \pm 2.77\%$ , respectively, averaged over the 13 cases. Among the 13 cases, chb02 and chb11 exhibited the highest accuracy of  $99.94 \pm 0.02\%$  (sensitivity and specificity of  $99.75 \pm 0.44\%$  and  $99.94 \pm 0.02\%$ ; 100% and  $99.94 \pm 0.02\%$ , respectively), whereas chb23 exhibited the lowest accuracy of  $93.92 \pm 8.54\%$  (sensitivity and specificity of  $87.49 \pm 21.67\%$  and  $93.96 \pm 8.61\%$ , respectively) averaged over  $k$ -fold cross-validation.

The seizure detection performance of the single-channel detectors in the event-level evaluation had a sensitivity, FAR, and latency of  $99.62 \pm 1.39\%$ ,  $0.22 \pm 0.34/h$ , and  $3.3 \pm 5.5s$ , averaged over the 13 cases, respectively. Single-channel seizure detection exhibited a mean number of correctly detected seizures, missed seizures, and false alarms of  $5.8 \pm 4.3$ ,  $0.1 \pm 0.3$ , and  $1.0 \pm 1.2$ , respectively, during a mean length of EEG recordings of  $7.0 \pm 4.1h$ . None of the cases exhibited an FAR higher than 1/h. Among the 13 cases, chb02 exhibited the highest FAR of 0.88/h with a sensitivity of 100%, whereas chb15 exhibited the lowest sensitivity (95%) with an FAR of 0.07/h.

Additionally, we performed single-channel seizure detection based on the publicly available annotations, to explore substantial effects of our re-annotation on the performance. The ictal-interictal

binary classification performance of our patient-specific single-channel seizure detectors trained using publicly available annotations in the segment-level evaluation had a sensitivity, specificity, accuracy, and AUC of  $96.39 \pm 2.75\%$ ,  $94.92 \pm 8.38\%$ ,  $94.93 \pm 8.35\%$ , and  $95.62 \pm 4.20\%$ , respectively, averaged over the 13 cases. Among the 13 cases, chb02 exhibited the highest accuracy of  $99.84 \pm 0.12\%$  (sensitivity and specificity of 100% and  $99.84 \pm 0.12\%$ , respectively), whereas chb17 exhibited the lowest accuracy of  $70.10 \pm 10.86\%$  (sensitivity and specificity of 100% and  $70.01 \pm 10.88\%$ , respectively), averaged over  $k$ -fold cross-validation.

The seizure detection performance of the single-channel detectors trained by the publicly available annotations in the event-level evaluation had a sensitivity, FAR, and latency of  $97.69 \pm 6.96\%$ ,  $0.16 \pm 0.26/h$ , and  $8.0 \pm 9.4s$ , averaged over the 13 cases, respectively. Single-channel seizure detection based on publicly available annotations exhibited a mean number of correctly detected seizures, missed seizures, and false alarms of  $5.8 \pm 4.4$ ,  $0.2 \pm 0.4$ , and  $1.2 \pm 2.1$ , respectively, during a mean length of EEG recordings of  $7.0 \pm 4.1h$ . None of the cases exhibited an FAR higher than 1/h. Among the 13 cases, chb02 exhibited the highest FAR of 0.88/h with a sensitivity of 100%, whereas chb04 exhibited the lowest sensitivity (75%) with an FAR of 0.09/h. Detailed results of the performances of our 18-, 4-, and single-channel seizure detectors averaged over the 13 cases are presented in Table 2 and Supplementary Tables S1–S4.

## 4 Discussion

We conducted patient-specific deep learning-based automated seizure detection in long-term scalp EEG recordings by reducing the number of channels from 18, 4 to 1, yielding a sensitivity of 97.05–100%, FAR of 0.22–0.40/h, and latency of 2.1–3.4 s averaged over the 13 cases of the CHB-MIT dataset. We obtained 18-channel seizure detectors with a full montage setting, 4-channel ones with two channels close to behind-the-ear positions and two channels at the forehead, and single-channel detectors with one specific channel among the four channels designated by the neurologists' confirmation of spatial seizure characteristics for individual patients. We examined that our single-channel detectors successfully identified seizures in long-term scalp EEG recordings comparable to our multi-channel detectors, thus suggesting the usefulness of our single-channel approach for wearable seizure detection in conjunction with neurologists' clinical designation of the most prominent seizure locations and its corresponding channel selection.

### 4.1 Previous seizure detection approach

Numerous studies have been suggested patient-specific deep learning-based automated seizure detection approaches using the CHB-MIT dataset (21, 34, 35, 37–48). In terms of seizure detection with a full montage setting, Xu et al. (44) proposed seizure detectors based on a three-dimensional (3D) CNN using time-frequency matrices by multiscale short-time Fourier transform with an average sensitivity, FAR, and latency of 94.95%, 0.08/h, and 2.3 s, respectively. Tang et al. (42) proposed a bidirectional long short-term memory (LSTM) network based on the attention mechanism and path signature algorithm yielding a seizure classification accuracy of

99.09%. Zhao et al. (48) proposed a hybrid attention network with graph modes and transformers yielding a seizure classification accuracy of 98.30%. Zhang et al. (47) proposed seizure detectors based on bidirectional gated recurrent units (GRUs) using time series decomposed by wavelet analysis, which exhibited an average sensitivity and FAR of 95.49% and 0.31/h, respectively. Wang et al. (35) proposed seizure detectors based on a stacked 1D CNN using multi-channel time series, which exhibited an average sensitivity, FAR, and latency of 99.31%, 0.20/h, and 8.1 s, respectively. Li et al. (41) proposed seizure detectors based on a CNN-LSTM hybrid architecture using multi-channel time series, which exhibited an average sensitivity and FAR of 95.29% and 0.66/h, respectively.

Despite the increase in the number of studies on full-montage seizure detectors, automated seizure detection with a reduced number of channels using the CHB-MIT dataset has been performed primarily using conventional machine learning techniques. Song et al. (49) proposed a channel screening method based on the refine composite multiscale dispersion entropy with residual convolutional LSTM yielding a seizure classification accuracy of 96.49% averaged over 14 subjects. However, this study had no result on the event-level evaluation. Tang et al. (21) proposed seizure detectors with five channels based on an autoencoder and support vector machine (SVM), yielding an average sensitivity, FAR, and latency of 97.2%, 0.64/h, and 1.1 s, respectively. Khanmohammadi et al. (40) proposed seizure detectors with five channels based on adaptive distancing, yielding an average sensitivity, FAR, and latency of 96%, 0.12/h, and 4.2 s, respectively. In the aforementioned studies, the channels were automatically selected using mathematical algorithms with amplitude variations or channel correlations. Rather than using channel-selection algorithms, a recent study manually selected specific channels that were expected to be important for seizure detection. Asif et al. (37) offered seizure detectors with 6–12 channels near the temporal lobe based on the random undersampling and boosting (RUSBoost), yielding an average sensitivity, FAR, and latency of 92%, 0.21/h, and 7.1 s, respectively, for their 10-channel detectors. They demonstrated the feasibility of using seizure detectors with a small number of channels in patients with temporal lobe epilepsy. In addition, they reported the performance of their 23-channel detectors with an average sensitivity, FAR, and latency of 95%, 0.16/h, and 6.8 s, respectively, suggesting an acceptable performance loss by channel reduction. Detailed information on the performance of previous studies using the CHB-MIT dataset for the event-level evaluation is presented in Table 3. Note that, in this study, our neurologists selected only one channel for single-channel seizure detection for each patient compared with other studies using less than full channel.

### 4.2 Proposed seizure detection approach

In this study, we built 18-channel detectors with a full montage setting that covered the entire scalp; 4-channel detectors with the smallest number of channels that could cover the frontal, temporal, parietal, and occipital regions; and single-channel detectors with one channel that could cover specific local area showing distinctive seizure characteristics. For our 4-channel detectors, the neurologists selected two channels, P7-O1 and P8-O2, which were closest to the behind-the-ear positions among the 18 channels in the international 10–20 system. They selected two additional channels, Fp1-F3 and Fp2-F4,

TABLE 2 Performance of patient-specific seizure detectors for ictal-interictal classification (segment-level) and seizure detection (event-level) averaged over the 13 cases by mean  $\pm$  standard deviation.

| Detector                                       | Segment-level evaluation |                  |                  |                  | Event-level evaluation |                 |               |                            |                |               |
|--|--------------------------|------------------|------------------|------------------|------------------------|-----------------|---------------|----------------------------|----------------|---------------|
|  | Sensitivity (%)          | Specificity (%)  | Accuracy (%)     | AUC (%)          | Sensitivity (%)        | FAR (/h)        | Latency (s)   | Correctly detected seizure | Missed seizure | False alarm   |
| 18-channel                                     | 98.66 $\pm$ 1.19         | 98.47 $\pm$ 2.71 | 98.47 $\pm$ 2.69 | 98.56 $\pm$ 1.81 | 100.00 $\pm$ 0.00      | 0.30 $\pm$ 0.47 | 2.1 $\pm$ 6.7 | 5.9 $\pm$ 4.6              | 0.0 $\pm$ 0.0  | 2.4 $\pm$ 4.4 |
| 4-channel                                      | 97.31 $\pm$ 3.78         | 97.72 $\pm$ 3.61 | 97.73 $\pm$ 3.59 | 97.51 $\pm$ 2.94 | 97.05 $\pm$ 9.23       | 0.40 $\pm$ 0.77 | 3.5 $\pm$ 4.8 | 5.8 $\pm$ 4.4              | 0.2 $\pm$ 0.4  | 2.9 $\pm$ 6.1 |
| Single-channel                                 | 96.76 $\pm$ 3.97         | 98.19 $\pm$ 1.82 | 98.18 $\pm$ 1.83 | 97.47 $\pm$ 2.77 | 99.62 $\pm$ 1.39       | 0.22 $\pm$ 0.34 | 3.3 $\pm$ 5.5 | 5.8 $\pm$ 4.3              | 0.1 $\pm$ 0.3  | 1.0 $\pm$ 1.2 |
| Single-channel (Publicly available annotation) | 96.39 $\pm$ 2.75         | 94.92 $\pm$ 8.38 | 94.93 $\pm$ 8.35 | 95.62 $\pm$ 4.20 | 97.69 $\pm$ 6.96       | 0.16 $\pm$ 0.26 | 8.0 $\pm$ 9.4 | 5.8 $\pm$ 4.4              | 0.2 $\pm$ 0.4  | 1.2 $\pm$ 2.1 |

An average EEG length for event-level evaluation is 7.0 $\pm$ 4.1 h. AUC and FAR denote area under the receiver operating characteristic curve and false alarm rate, respectively.

close to the forehead to detect seizures occurring in the frontal region. We had several reasons for the selection of the four channels as follows: first, behind-the-ear EEG monitoring was a well-known wearable approach, considering temporal lobe seizures known as the most common focal ones (26, 28, 50); second, it could be challenging for the behind-the-ear monitoring to cover frontal regions; and third, both the behind-the-ear and forehead positions were expected to be suitable for easily attaching electrodes owing to minimal amount of hair. In terms of our single-channel approach, we can consider a situation in which neurologists provide single-channel seizure detection systems to patients with refractory epilepsy after confirming the most critical seizure-generating regions on the patient’s scalp. Thus, patients can use their systems comfortably with only one channel for a long period. No channel selection algorithm was used for our 4- and single-channel detectors because we intended to adopt only the neurologists’ clinical opinions. We observed that the performance of our single-channel seizure detector was comparable to that of other studies, as presented in Table 3. Channel selection methods of previous studies using the CHB-MIT dataset in comparison with our single-channel seizure detection approach is shown in Supplementary Table S5.

Overall, we confirmed that no significant difference existed in detection abilities with respect to the number of channels. However, we observed that, in some cases, the number of channels had some influence on the seizure detection performance in the event-level evaluation. We examined the cases having differences in the false alarms  $\geq 2$  and the latency  $\geq 3$  s. Two cases of chb02 and chb08 showed an increase, whereas four cases of chb03, chb10, chb11, and chb15 showed a decrease in the number of false alarms for single-channel seizure detection compared with multi-channel one. Two cases of chb05 and chb17 showed an increase, whereas chb15 showed a decrease in the latency for single-channel seizure detection compared with multi-channel one. In particular, chb15 showed remarkable increases in the performance in terms of both the false alarms and latency. We suggest that single-channel seizure detection can exclude artifact-contaminated or unnecessary channels, possibly resulting in the reduction of the number of false alarms and the latency using less contaminated training datasets. However, there may be any loss of information on inter-channel relationships which can affect seizure detection ability. Therefore, further studies on how spatial epileptic EEG features vary in accordance with the number of channels in individual cases. Figure 4 shows a representative single-channel seizure detection based on our event-level evaluation for the second seizure of chb11. It describes that our single-channel detector using P7-O1 designated by the neurologists as the most prominent seizure location provides the best performance compared with others. That using Fp1-F3 also detects the seizure, but it generates more ictal probabilities potentially inducing false alarms. Single-channel seizure detection performance of chb11 in accordance with four channels is shown in Supplementary Table S6.

### 4.3 Wearable seizure detection

Recent studies have proposed patient-specific automated wearable seizure detection approaches using 4-channel behind-the-ear scalp EEG recordings with deep learning and machine learning techniques to achieve real-time identification of seizures in long-term EEG

TABLE 3 Seizure detection performance of previous studies using the CHB-MIT dataset in comparison with ours.

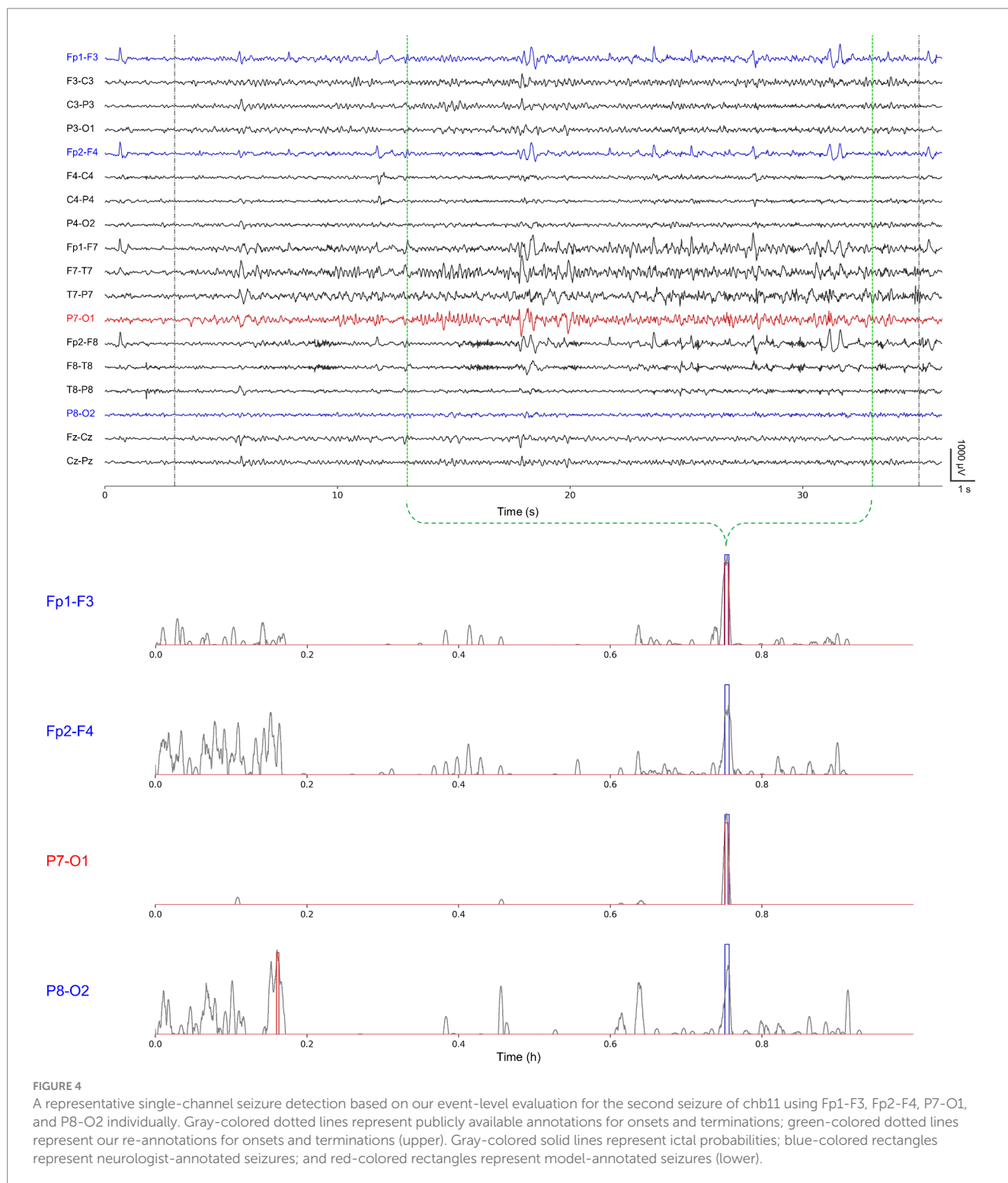
| Study                   | Number of channels                  | Input data   | Deep/machine learning   | Sensitivity (%)  | FAR (/h)   | Latency (s)  |
|-------------------------|-------------------------------------|--|---|--|--|--|
| Y. Xu et al.            | Full                                | Multiscale STFT  | 3D-CNN  | 94.95  | 0.08   | 2.3  |
| Y. Zhang et al.         | Full                                | Time series decomposition by DWT   | <ul style="list-style-type: none"> <li>• Bi-GRU</li> <li>• GRU</li> </ul> | <ul style="list-style-type: none"> <li>• 95.49 (Bi-GRU)</li> <li>• 92.96 (GRU)</li> </ul>          | <ul style="list-style-type: none"> <li>• 0.31</li> <li>• 0.57</li> </ul> |  |
| X. Wang et al.          | Full                                | Time series  | Stacked 1D-CNN  | 99.31  | 0.20   | 8.1  |
| Y. Li et al.            | Full                                | Time series  | CNN-LSTM  | 95.29  | 0.66   |  |
| Y. Guo et al.           | Full                                | Time series decomposition by DWT   | EasyEnsemble  | 97.50 ~ 100  | 0.91 ~ 1.38  |  |
| R. Zanetti et al.       | Full                                | Approximate zero-crossing  | Random forest   | 77.27  | 0.09   |  |
| L. S. Vidyaratne et al. | Full                                | <ul style="list-style-type: none"> <li>• Fractal dimension estimation</li> <li>• Harmonic wavelet packet transform</li> </ul>            | Relevance vector machine  | 96.00  | 0.10   | 1.9  |
| M. Zabihi et al.        | Full                                | Phase space reconstruction   | LDA and Naive Bayes   | 91.34 ~ 96.29  | 3.04 ~ 4.86  | 4.65 ~ 5.03  |
| B. Hunyadi et al.       | Full                                | Feature-channel matrix   | SVM   | 80 ~ 83  | 0.41 ~ 0.88  | 8.5 ~ 10.0   |
| A. Shueb et al.         | Full                                | Time series decomposition by DWT   | SVM   | 96.00  | 0.08   | Among 173 seizures, <ul style="list-style-type: none"> <li>• &lt;3 s (50%)</li> <li>• &lt;5 s (71%)</li> <li>• &lt;10 s (91%)</li> </ul> |
| F.-G. Tang et al.       | 5                                   | <ul style="list-style-type: none"> <li>• Time series decomposition by DWT</li> <li>• Frequency-domain features by autoencoder</li> </ul> | SVM   | 97.20  | 0.64   | 1.1  |
| R. Asif et al.          | 6, 8, 10, and 12 on temporal region | Time-domain statistical features   | RUSBoost  | <ul style="list-style-type: none"> <li>• 95 (full channels)</li> <li>• 92 (10 channels)</li> </ul> | <ul style="list-style-type: none"> <li>• 0.16</li> <li>• 0.21</li> </ul> | <ul style="list-style-type: none"> <li>• 6.83</li> <li>• 7.1</li> </ul>  |
| S. Khanmohammadi et al. | 5                                   | <ul style="list-style-type: none"> <li>• Time domain statistical features</li> <li>• Spectral power</li> </ul>                           | Adaptive distance-based change point detector                             | 96.00  | 0.12   | 4.2  |
| This study              | 18                                  | Time series  | Stacked 2D-CNN  | 100.00   | 0.30   | 2.1  |
|                         | 4                                   | Time series  | Stacked 2D-CNN  | 97.05  | 0.40   | 3.4  |
|                         | Single                              | Time series  | Stacked 2D-CNN  | 99.62  | 0.22   | 3.3  |

Full in the column of number of channels represents ≥18 channels. STFT and DWT in the column of input data denote short-time Fourier transform and discrete wavelet transform, respectively. CNN, GRU, LSTM, LDA, SVM, and RUSBoost denote convolutional neural network, gated recurrent unit, long short-term memory, linear discriminant analysis, support vector machine, and random undersampling and boosting, respectively. FAR denotes false alarm rate.

recordings. You et al. (28) reported an average sensitivity and FAR of 94.2% and 0.29/h, respectively, for their variational autoencoder-based approaches. Zhang et al. (27) reported an average sensitivity and FAR of 87.5% and 1.93/h, respectively; Swinnen et al. (25) reported 98.3% and 0.91/h, respectively; Vandecasteele et al. (26) reported 69.1% and 0.02/h, respectively; and Gu et al. (24) reported 94.5% and 0.52/h, respectively, for their SVM-based approaches. They suggested that behind-the-ear EEG monitoring was highly convenient, particularly for patients requiring continuously examination in out-of-hospital settings. However, we were concerned that seizure-detection approaches using the behind-the-ear channels could be mostly focused on the seizures occurring near the temporal lobe. Other recent studies utilized a single-channel EEG sensor called Epilog for the feasibility of long-term wearable seizure detection outside the hospital. Frankel et al. (31) demonstrated that epileptologists could successfully identify seizures in single-channel

EEG recordings when the sensors were placed near the seizure onset foci with an accuracy higher than 80%. They (30) also reported a random forest-based seizure detection approach using single-channel EEG recordings with an average sensitivity and FAR of 87.5% and 0.14/h, respectively.

As we used the CHB-MIT dataset, comparing the performance of our study with that of the aforementioned studies was challenging. However, in terms of wearable seizure detection, we believe that this study has two key strengths compared with the previous ones as follows: first, neurologists select the most prominent seizure location for each patient from the 18-channel longitudinal bipolar montage in accordance with the international 10–20 system after reviewing electroencephalographic seizure signatures directly; second, our single-channel approach is expected to be applicable to both focal and generalized seizures due to the use of the aforementioned neurologist-selected channel for each patient regardless of the seizure types.



### 4.4 Seizure re-annotation

Instead of using publicly available annotations in the CHB-MIT dataset as in previous studies, we modified the annotations based on our neurologists' re-examination of seizure onsets and terminations for the following two reasons. First, we needed to

determine which region of the scalp had the most distinct seizure characteristics and which channel could be the most important for single-channel seizure detection in individual patients. For this purpose, we shifted the positions of seizure onsets and terminations to disclose spatial seizure characteristics as clearly as possible. Second, we intended to obtain training data for our classification

models that were less contaminated than those from publicly available annotations. We assumed that our single-channel detectors would be stable for unseen data, which was in line with a previous study on the robustness of deep neural networks with a sufficient volume of cleanly labeled data (51).

In our results, chb17 showed a remarkable increase of >26% on average in the specificity of its classification models based on our re-annotations. In the event-level evaluation, six cases of chb04, chb05, chb07, chb08, chb15, and chb22 showed a decrease in the latency ( $\geq 3$  s). Additionally, two cases of chb10 and chb15 exhibited a decrease in the false alarms ( $\geq 2$ ). Particularly, chb15 exhibited a marked reduction in the number of false alarms using our re-annotations. We suggest that our re-annotations will benefit some cases, particularly those with considerably high latency and false alarms in single-channel seizure detection. Similarly, a previous study reported significant performance enhancement in wearable EEG-based seizure detection with automatic annotation correction (27). However, two cases of chb08 and chb11 showed an increase in the false alarms ( $\geq 2$ ). Further studies are required to understand the possible negative effects of our re-annotations on seizure detection.

#### 4.5 Limitations and future research

This study has some limitations. First, we used patient-specific seizure detection approaches. Numerous recent studies on patient-independent seizure detection approaches have shown high performance with sensitivity >85% and FAR<0.5/h with a full montage setting using the CHB-MIT dataset (52–54). A patient-independent approach is required to establish the generalizability of our single-channel seizure detection. Second, we adopted a 2D CNN architecture with two 2D CNN modules stacked in parallel to efficiently extract time-varying electroencephalographic signatures using two types of filter lengths, similar to the previous study on stacked 1D CNN-based seizure detection (35). However, other studies have adopted other deep-learning methods, such as 3D CNNs (44), transformers (48), GRUs (47), and a hybrid of CNN and LSTM (41) with the CHB-MIT dataset. Therefore, we must perform single-channel seizure detection using other deep-learning techniques and examine their computational complexity. Moreover, we need to carry out feature analysis studies based on explainable deep learning methods to understand possible reasons for falsely detected and missed seizures to improve our single-channel seizure detection performance. Third, we empirically set the post-processing parameters in the event-level evaluation to maximize the seizure detection performance for each patient. As a trade-off exists between sensitivity and FAR, the parameters should be carefully tuned for each patient to avoid erroneous detection as much as possible. Therefore, we must consider more systematic designs to optimize the parameters, such as adaptive thresholding, to reflect seizure patterns and tunable artifact rejection, and reduce excessive false alarms (55–57). Finally, to strengthen our findings and to validate our approaches' effectiveness, we must increase the number of patients through other open datasets or collaborative multicenter studies beyond the 13 patients in the CHB-MIT

dataset. However, we need to carefully concern that larger studies demand higher time and cost consumption.

## 5 Conclusion

We constructed patient-specific deep learning-based 18-, 4-, and single-channel automated seizure detectors using long-term scalp EEG recordings from the CHB-MIT dataset by reducing the number of EEG channels. Note that neurologists selected a specific channel based on the spatial seizure characteristics of individual patients among the four channels in which two were close to the behind-the-ear regions, and the other two were at the frontal lobe for our single-channel detectors. The seizure detection performance of our single-channel detectors achieved an average sensitivity of >99% and FAR of <0.3/h, which were comparable to those of our multi-channel detectors. In addition, the re-annotation of well-characterized seizures could partially improve the performance of single-channel seizure detection, particularly for false alarms and latency. We suggest that our single-channel approach in conjunction with neurologists' clinical designation of the most prominent seizure locations has a high potential for application in wearable devices for seizure detection in long-term EEG recordings for patients with refractory epilepsy.

## Data availability statement

Publicly available datasets were analyzed in this study. This data can be found here: the Children's Hospital Boston-Massachusetts Institute of Technology (CHB-MIT) scalp EEG database repository, <https://physionet.org/content/chbmit/1.0.0/>.

## Ethics statement

The study involving humans was approved by the Institutional Review Board of Seoul National University Bundang Hospital (No. B-2205-758-105). The study was conducted in accordance with the local legislation and institutional requirements. The ethics committee/institutional review board waived the requirement of written informed consent for participation from the participants or the participants' legal guardians/next of kin because of the retrospective nature of the study.

## Author contributions

YC: Data curation, Formal analysis, Methodology, Software, Validation, Visualization, Writing – original draft, Writing – review & editing. AC: Conceptualization, Data curation, Investigation, Methodology, Visualization, Writing – review & editing. HK: Conceptualization, Data curation, Formal analysis, Funding acquisition, Investigation, Methodology, Project administration, Resources, Supervision, Validation, Visualization, Writing – original draft, Writing – review & editing. KK: Conceptualization, Investigation, Methodology, Writing – review & editing.

## Funding

The authors declare that financial support was received for the research, authorship, and/or publication of this article. This study was supported by SK Biopharmaceuticals Co., Ltd. under Grant No. 06–2022-0189. The funder was not involved in the study design, collection, analysis, interpretation of data, the writing of this article, or the decision to submit it for publication.

## Conflict of interest

The authors declare that the research was conducted in the absence of any commercial or financial relationships that could be construed as a potential conflict of interest.

## References

1. Fiest KM, Sauro KM, Wiebe S, Patten SB, Kwon CS, Dykeman J, et al. Prevalence and incidence of epilepsy: a systematic review and meta-analysis of international studies. *Neurology*. (2017) 88:296–303. doi: 10.1212/WNL.0000000000003509
2. Chang BS, Lowenstein DH. Epilepsy. *N Engl J Med*. (2003) 349:1257–66. doi: 10.1056/NEJMra022308
3. Kwan P, Brodie MJ. Early identification of refractory epilepsy. *N Engl J Med*. (2000) 342:314–9. doi: 10.1056/NEJM200002033420503
4. Moshe SL, Perucca E, Ryvlin P, Tomson T. Epilepsy: new advances. *Lancet*. (2015) 385:884–98. doi: 10.1016/S0140-6736(14)60456-6
5. Noachtar S, Remi J. The role of EEG in epilepsy: a critical review. *Epilepsy Behav*. (2009) 15:22–33. doi: 10.1016/j.yebeh.2009.02.035
6. Kwan P, Schachter SC, Brodie MJ. Drug-resistant epilepsy. *N Engl J Med*. (2011) 365:919–26. doi: 10.1056/NEJMra1004418
7. Laxer KD, Trinka E, Hirsch LJ, Cendes F, Langfitt J, Delanty N, et al. The consequences of refractory epilepsy and its treatment. *Epilepsy Behav*. (2014) 37:59–70. doi: 10.1016/j.yebeh.2014.05.031
8. Chayasirisobhon S, Griggs L, Westmoreland S, Kim CS. The usefulness of one to two hour video EEG monitoring in patients with refractory seizures. *Clin Electroencephalogr*. (1993) 24:78–84. doi: 10.1177/155005949302400208
9. Ghougassian DE, D'souza W, Cook MJ, O'Brien TJ. Evaluating the utility of inpatient video-EEG monitoring. *Epilepsia*. (2004) 45:928–32. doi: 10.1111/j.0013-9580.2004.51003.x
10. Riquet A, Lamblin MD, Bastos M, Bulteu C, Derambure P, Vallee L, et al. Usefulness of video-EEG monitoring in children. *Seizure*. (2011) 20:18–22. doi: 10.1016/j.seizure.2010.09.011
11. Cherian R, Kanaga EG. Theoretical and methodological analysis of EEG based seizure detection and prediction: an exhaustive review. *J Neurosci Methods*. (2022) 369:109483. doi: 10.1016/j.jneumeth.2022.109483
12. Ganguly TM, Ellis CA, Tu D, Shinohara RT, Davis KA, Litt B, et al. Seizure detection in continuous inpatient EEG: a comparison of human vs automated review. *Neurology*. (2022) 98:e2224–32. doi: 10.1212/WNL.00000000000200267
13. Shoeibi A, Moridian P, Khodatars M, Ghassemi N, Jafari M, Alizadehsani R, et al. An overview of deep learning techniques for epileptic seizures detection and prediction based on neuroimaging modalities: methods, challenges, and future works. *Comput Biol Med*. (2022) 149:106053. doi: 10.1016/j.combiomed.2022.106053
14. Avcu MT, Zhang Z, Chan DWS. Seizure detection using least EEG channels by deep convolutional neural network. In: *IEEE international conference on acoustics, speech and signal processing*. Brighton, UK: IEEE (2019)
15. Gabeff V, Teijeiro T, Zapater M, Cammoun L, Rheims S, Ryvlin P, et al. Interpreting deep learning models for epileptic seizure detection on EEG signals. *Artif Intell Med*. (2021) 117:102084. doi: 10.1016/j.artmed.2021.102084
16. Hartmann M, Koren J, Baumgartner C, Duun-Henriksen J, Gritsch G, Kluge T, et al. Seizure detection with deep neural networks for review of two-channel electroencephalogram. *Epilepsia*. (2022) 64 Suppl 4:S34–9. doi: 10.1111/epi.17259
17. Maher C, Yang Y, Truong ND, Wang C, Nikpour A, Kavehei O. Towards long term monitoring: seizure detection with reduced electroencephalogram channels. *Med Rxiv*. (2021). doi: 10.1101/2021.12.14.21267701
18. Ozdemir MA, Cura OK, Akan A. Epileptic EEG classification by using time-frequency images for deep learning. *Int J Neural Syst*. (2021) 31:2150026. doi: 10.1142/S012906572150026X
19. Pisano F, Sias G, Fanni A, Cannas B, Dourado A, Pisano B, et al. Convolutional neural network for seizure detection of nocturnal frontal lobe epilepsy. *Complexity*. (2020) 2020:1–10. doi: 10.1155/2020/4825767

## Publisher's note

All claims expressed in this article are solely those of the authors and do not necessarily represent those of their affiliated organizations, or those of the publisher, the editors and the reviewers. Any product that may be evaluated in this article, or claim that may be made by its manufacturer, is not guaranteed or endorsed by the publisher.

## Supplementary material

The Supplementary material for this article can be found online at: <https://www.frontiersin.org/articles/10.3389/fneur.2024.1389731/full#supplementary-material>

20. Shah V, Golmohammadi M, Ziyabari S, Von Weltin E, Obeid I, Picone J. Optimizing channel selection for seizure detection. In: *IEEE signal processing in medicine and biology symposium*. Philadelphia, PA, USA: IEEE (2017)
21. Tang F-G, Liu Y, Li Y, Peng Z-W. A unified multi-level spectral-temporal feature learning framework for patient-specific seizure onset detection in EEG signals. *Knowl Based Syst*. (2020) 205:106152. doi: 10.1016/j.knsys.2020.106152
22. Yuan Y, Xun G, Jia K, Zhang A. A multi-view deep learning framework for EEG seizure detection. *IEEE J Biomed Health Inform*. (2019) 23:83–94. doi: 10.1109/JBHI.2018.2871678
23. Zhang B, Wang W, Xiao Y, Xiao S, Chen S, Chen S, et al. Cross-subject seizure detection in EEGs using deep transfer learning. *Comput Math Methods Med*. (2020) 2020:1–8. doi: 10.1155/2020/7902072
24. Gu Y, Cleeren E, Dan J, Claes K, Van Paesschen W, Van Huffel S, et al. Comparison between scalp EEG and behind-the-ear EEG for development of a wearable seizure detection system for patients with focal epilepsy. *Sensors*. (2018) 18:29. doi: 10.3390/s18010029
25. Swinnen L, Chatzichristos C, Jansen K, Lagae L, Depondt C, Seynaeve L, et al. Accurate detection of typical absence seizures in adults and children using a two-channel electroencephalographic wearable behind the ears. *Epilepsia*. (2021) 62:2741–52. doi: 10.1111/epi.17061
26. Vandecasteele K, De Cooman T, Dan J, Cleeren E, Van Huffel S, Hunyadi B, et al. Visual seizure annotation and automated seizure detection using behind-the-ear electroencephalographic channels. *Epilepsia*. (2020) 61:766–75. doi: 10.1111/epi.16470
27. Zhang J, Chatzichristos C, Vandecasteele K, Swinnen L, Broux V, Cleeren E, et al. Automatic annotation correction for wearable EEG based epileptic seizure detection. *J Neural Eng*. (2022) 19:016038. doi: 10.1088/1741-2552/ac54c1
28. You S, Hwan Cho B, Shon YM, Seo DW, Kim IY. Semi-supervised automatic seizure detection using personalized anomaly detecting variational autoencoder with behind-the-ear EEG. *Comput Methods Prog Biomed*. (2022) 213:106542. doi: 10.1016/j.cmpb.2021.106542
29. Zibrantsen IC, Kidmose P, Christensen CB, Kjaer TW. Ear-EEG detects ictal and interictal abnormalities in focal and generalized epilepsy - a comparison with scalp EEG monitoring. *Clin Neurophysiol*. (2017) 128:2454–61. doi: 10.1016/j.clinph.2017.09.115
30. Frankel MA, Lehmkuhle MJ, Spitz MC, Newman BJ, Richards SV, Arain AM. Wearable reduced-channel EEG system for remote seizure monitoring. *Front Neurol*. (2021) 12:728484. doi: 10.3389/fneur.2021.728484
31. Frankel MA, Lehmkuhle MJ, Watson M, Fetrow K, Frey L, Drees C, et al. Electrographic seizure monitoring with a novel, wireless, single-channel EEG sensor. *Clin Neurophysiol Pract*. (2021) 6:172–8. doi: 10.1016/j.cnp.2021.04.003
32. Gotman J. Automatic recognition of epileptic seizures in the EEG. *Electroencephalogr Clin Neurophysiol*. (1982) 54:530–40. doi: 10.1016/0013-4694(82)90038-4
33. Shoeb A, Edwards H, Connolly J, Bourgeois B, Treves ST, Guttig J. Patient-specific seizure onset detection. *Epilepsy Behav*. (2004) 5:483–98. doi: 10.1016/j.yebeh.2004.05.005
34. Shoeb A, Guttig J. Application of machine learning to epileptic seizure detection. In: *Proceedings of the 27th international conference on international conference on machine learning* (2010). 975–82.
35. Wang X, Wang X, Liu W, Chang Z, Karkkainen T, Cong F. One dimensional convolutional neural networks for seizure onset detection using long-term scalp and intracranial EEG. *Neurocomputing*. (2021) 459:212–22. doi: 10.1016/j.neucom.2021.06.048

36. Savitzky A, Golay MJE. Smoothing and differentiation of data by simplified least squares procedures. *Anal Chem.* (1964) 36:1627–39. doi: 10.1021/ac60214a047
37. Asif R, Saleem S, Hassan SA, Alharbi SA, Kamboh AM. Epileptic seizure detection with a reduced montage: a way forward for ambulatory EEG devices. *IEEE Access.* (2020) 8:65880–90. doi: 10.1109/ACCESS.2020.2983917
38. Guo Y, Jiang X, Tao L, Meng L, Dai C, Long X, et al. Epileptic seizure detection by cascading isolation forest-based anomaly screening and easy ensemble. *IEEE Trans Neural Syst Rehabil Eng.* (2022) 30:915–24. doi: 10.1109/TNSRE.2022.3163503
39. Hunyadi B, Signoretto M, Van Paesschen W, Suykens JA, Van Huffel S, De Vos M. Incorporating structural information from the multichannel EEG improves patient-specific seizure detection. *Clin Neurophysiol.* (2012) 123:2352–61. doi: 10.1016/j.clinph.2012.05.018
40. Khanmohammadi S, Chou CA. Adaptive seizure onset detection framework using a hybrid PCA-CSP approach. *IEEE J Biomed Health Inform.* (2018) 22:154–60. doi: 10.1109/JBHI.2017.2703873
41. Li Y, Yu Z, Chen Y, Yang C, Li Y, Allen Li X, et al. Automatic seizure detection using fully convolutional nested LSTM. *Int J Neural Syst.* (2020) 30:2050019. doi: 10.1142/S0129065720500197
42. Tang Y, Wu Q, Mao H, Guo L. Epileptic seizure detection based on path signature and bi-LSTM network with attention mechanism. *IEEE Trans Neural Syst Rehabil Eng.* (2024) 32:304–13. doi: 10.1109/TNSRE.2024.3350074
43. Vidyaratne LS, Iftekharuddin KM. Real-time epileptic seizure detection using EEG. *IEEE Trans Neural Syst Rehabil Eng.* (2017) 25:2146–56. doi: 10.1109/TNSRE.2017.2697920
44. Xu Y, Yang J, Ming W, Wang S, Sawan M. Shorter latency of real-time epileptic seizure detection via probabilistic prediction. *Expert Syst Appl.* (2024) 236:121359. doi: 10.1016/j.eswa.2023.121359
45. Zabihi M, Kiranyaz S, Rad AB, Katsaggelos AK, Gabbouj M, Ince T. Analysis of high-dimensional phase space via Poincare section for patient-specific seizure detection. *IEEE Trans Neural Syst Rehabil Eng.* (2016) 24:386–98. doi: 10.1109/TNSRE.2015.2505238
46. Zanetti R, Pale U, Teijeiro T, Atienza D. Approximate zero-crossing: a new interpretable, highly discriminative and low-complexity feature for EEG and iEEG seizure detection. *J Neural Eng.* (2022) 19:066018. doi: 10.1088/1741-2552/acale4
47. Zhang Y, Yao S, Yang R, Liu X, Qiu W, Han L, et al. Epileptic seizure detection based on bidirectional gated recurrent unit network. *IEEE Trans Neural Syst Rehabil Eng.* (2022) 30:135–45. doi: 10.1109/TNSRE.2022.3143540
48. Zhao Y, He J, Zhu F, Xiao T, Zhang Y, Wang Z, et al. Hybrid attention network for epileptic EEG classification. *Int J Neural Syst.* (2023) 33:2350031. doi: 10.1142/S0129065723500314
49. Song Y, Fan C, Mao X. Optimization of epilepsy detection method based on dynamic EEG channel screening. *Neural Netw.* (2024) 172:106119. doi: 10.1016/j.neunet.2024.106119
50. Vinti V, Dell'isola GB, Tascini G, Mencaroni E, Cara GD, Striano P, et al. Temporal lobe epilepsy and psychiatric comorbidity. *Front Neurol.* (2021) 12:775781. doi: 10.3389/fneur.2021.775781
51. Rolnick D, Veit A, Belongie S, Shavit N. "Deep learning is robust to massive label noise". (arXiv:1705.10694v3 [cs.LG]). (2018). Cornell Tech (maintained and operated by Cornell Tech).
52. Liu G, Tian L, Zhou W. Patient-independent seizure detection based on channel-perturbation convolutional neural network and bidirectional long short-term memory. *Int J Neural Syst.* (2022) 32:2150051. doi: 10.1142/S0129065721500519
53. Thodoroff P, Pineau J, Lim A. (2016). "Learning robust features using deep learning for automatic seizure detection". (arXiv:1608.00220 [cs.LG]).
54. Wei Z, Zou J, Zhang J, Xu J. Automatic epileptic EEG detection using convolutional neural network with improvements in time-domain. *Biomed Signal Process Control.* (2019) 53:101551. doi: 10.1016/j.bspc.2019.04.028
55. Hopfengartner R, Kasper BS, Graf W, Gollwitzer S, Kreiselmeyer G, Stefan H, et al. Automatic seizure detection in long-term scalp EEG using an adaptive thresholding technique: a validation study for clinical routine. *Clin Neurophysiol.* (2014) 125:1346–52. doi: 10.1016/j.clinph.2013.12.104
56. Hopfengartner R, Kerling F, Bauer V, Stefan H. An efficient, robust and fast method for the offline detection of epileptic seizures in long-term scalp EEG recordings. *Clin Neurophysiol.* (2007) 118:2332–43. doi: 10.1016/j.clinph.2007.07.017
57. Kelly KM, Shiao DS, Kern RT, Chien JH, Yang MC, Yandora KA, et al. Assessment of a scalp EEG-based automated seizure detection system. *Clin Neurophysiol.* (2010) 121:1832–43. doi: 10.1016/j.clinph.2010.04.016